Article

Enantiopure [Cs+/Xe#Cryptophane]#FeII4L4 Hierarchical Superstructures

Dawei Zhang, Tanya K Ronson, Jake L. Greenfield, Thierry Brotin, Patrick Berthault, Estelle Leonce, Junlong Zhu, Lin Xu, and Jonathan R. Nitschke

Just Accepted

Enantiopure [Cs$^+$/Xe⊂Cryptophane]⊂Fe$^{II}_4$L$_4$ Hierarchical Superstructures

Dawei Zhang,[†] Tanya K. Ronson,[†] Jake L. Greenfield,[†] Thierry Brotin,[‡] Patrick Berthault,[§]

Estelle Léonce,[§] Junlong Zhu,[#] Lin Xu,[†,#] and Jonathan R. Nitschke*,[†]

[†]*Department of Chemistry, University of Cambridge, Lensfield Road, Cambridge CB2 1EW, UK.*

[‡]*Lyon 1 University, Ecole Normale Supérieure de Lyon, CNRS UMR 5182, Laboratoire de chimie, 69364 Lyon, France.*

[§]*NIMBE, CEA, CNRS, Université de Paris Saclay, CEA Saclay, 91191 Gif-sur-Yvette, France.*

[#]*Shanghai Key Laboratory of Green Chemistry and Chemical Processes, School of Chemistry and Molecular Engineering, East China Normal University, Shanghai 200062, China.*

Abstract

Hierarchically nested hosts offer new opportunities to control the guest binding of the inner host, functionalize the cavity of the outer host, and investigate communication between different layers. Here we report a self-assembled triazatruxene-based Fe$^{II}_4$L$_4$ capsule, which was able to encapsulate a covalent cage, cryptophane-111 (CRY). The resulting cage-in-cage complex was capable of accommodating a cesium cation or xenon atom with altered guest binding behavior compared to the CRY alone. A crystal structure of the Russian doll complex [Cs$^+$⊂CRY]⊂Fe$^{II}_4$L$_4$ unambiguously demonstrated the unusual encapsulation of a cation within a capsule bearing a 8+ charge. Moreover, the binding of enantiopure CRY occurred with high enantioselectivity (530-fold) between the two enantiomers of the tetrahedron. This discrimination resulted in stereochemical information transfer from the inner covalent cage to the outer self-assembled capsule, leading to the formation of enantiopure [guest⊂cage]⊂cage complexes. The

stereochemistry of the tetrahedron persisted even after displacement of CRY with an achiral guest.

Introduction

Russian-doll-like superstructures[1] consisting of nested host-in-host complexes[2] as essential precursors, have intrigued supramolecular chemists for over a decade.[3] Besides the beauty of the hierarchical architectures, the binding properties of the inner host, ensconced within the outer host, may be changed through outer-host encapsulation.[1d,1g,4] This effect evokes the encapsulation of enzymes in nanometer-sized protein compartments to enhance and control enzymatic activity.[5] This strategy also offers a new approach to internally functionalize larger capsules,[6] endowing them with the ability to bind molecules that are not otherwise encapsulated. These newly designed Russian dolls, which consist of robust, multiple three-dimensional nested hosts, thus compliment and build upon the foundations of those involving two-dimensional macrocycles[1a-j,1l] or single assemblies with multi-layered walls.[1k,2e,2f]

Coordination-driven self-assembled capsules[7] are excellent outer hosts because they may be designed to be large and to have wide-ranging guest binding abilities. They also exhibit structural adaptability as a consequence of the reversibility of their coordinative bonds.[8] In contrast, cryptophanes,[9] a type of covalent cage built from two cyclotribenzylene units,[10] serve very well as inner hosts. They encapsulate small molecules such as methane or xenon, as well as cations and anions.[9] Furthermore, many cryptophanes are inherently chiral.[9] When used in enantiopure form, they enable the investigation of the stereochemical communication between the different layers of Russian doll complexes, allowing a new class of enantiopure nested hosts to be investigated.

Here we show the encapsulation of cryptophane-111 (CRY)[11] within a self-assembled $Fe^{II}_4L_4$ capsule constructed from a triazatruxene-based subcomponent, and demonstrate how cage-in-cage formation alters the binding behavior of the inner cage and endows the outer tetrahedron

Journal of the American Chemical Society

with new binding ability. Cesium cations and xenon atoms are bound within the host-in-host complex to form Russian doll-like superstructures. Stereochemical communication occurred between layers when enantiopure CRY was employed, resulting in the handedness of the tetrahedron host framework becoming fixed by the CRY guest stereochemistry and allowing further fabrication of enantiopure three-component Russian doll complexes. The stereochemical configuration of the outer host was robustly maintained even following the displacement of the CRY by an achiral guest.

Results and Discussion

Triazatruxene-based subcomponent **A** was synthesized in four steps from commercially available starting materials (Figure S1). The reaction of subcomponent **A** (4 equiv) with iron(II) bis(trifluoromethanesulfonyl)imide (triflimide, Tf_2N^-) (4 equiv) and 2-formylpyridine (12 equiv) in acetonitrile afforded tetrahedron **1** with one triazatruxene capping each face (Figure 1). The $Fe^{II}_4L_4$ composition of the assembly was confirmed by ESI-MS (Figure S12). Due to the possibility of either clockwise (C) or anticlockwise (A) orientation of the triazatruxene panels around the center of each face, as well as the Λ or Δ handedness at the tris-chelated octahedral vertices of the tetrahedron, a series of stereoisomers might be envisaged.[12] The ^{1}H NMR spectrum of $Fe^{II}_4L_4$ **1** displayed only one set of ligand signals (Figure 1), suggesting the exclusive formation of a pair of *T*-symmetric tetrahedral enantiomers with homochiral faces and vertices. We infer that the homochiral configuration of **1** arises from the rigid three-fold symmetric ligands, which provide conformational rigidity to the cage framework, as has been observed for cages built from other C_3-symmetric ligands.[13] Based upon the crystal structure discussed below, we infer these to be $A_4\Delta_4$-**1** and $C_4\Lambda_4$-**1**, with anticlockwise (*A*) triazatruxene panels always paired with Δ handedness of the iron(II) stereocenters, and clockwise (*C*) triazatruxene with Λ iron(II). We thus refer to these stereoisomers as Δ_4-**1** and Λ_4-**1**, henceforth.
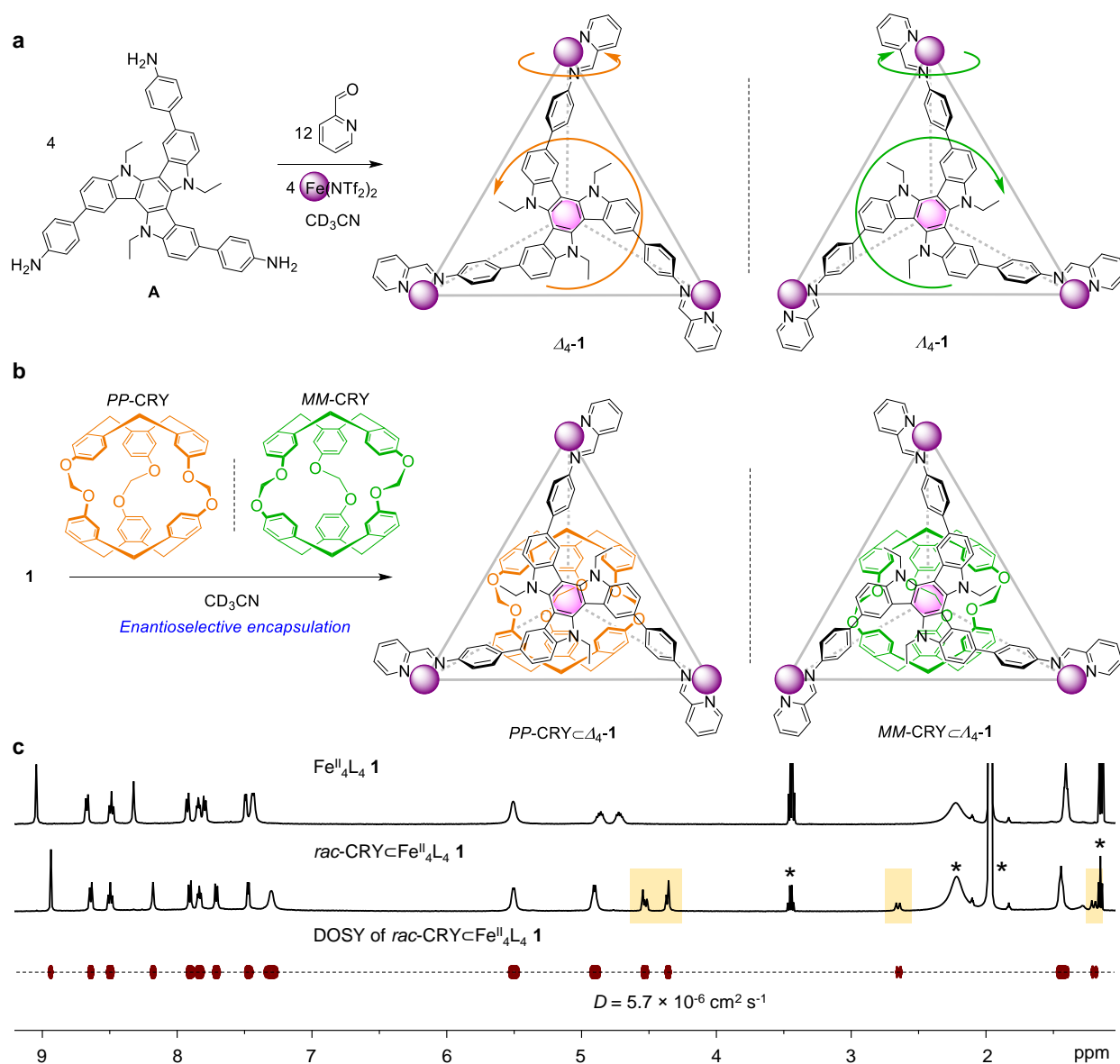
Figure 1. (a) Subcomponent self-assembly of **1**. (b) Enantioselective encapsulation of *rac*-CRY by **1**. (c) ¹H NMR spectra (CD₃CN, 500 MHz, 25 °C) of **1** and CRY⊂**1**, and DOSY spectrum of CRY⊂**1**. The peaks of the encapsulated CRY have been highlighted with a light orange background. Solvent peaks from diethyl ether, water and acetonitrile are indicated by asterisks. DOSY NMR indicated that the signals from **1** and the bound CRY diffuse at the same rate.

Addition of racemic CRY (*rac*-CRY) to a solution of **1** in acetonitrile led to formation of the cage-in-cage complex, CRY⊂**1**, after 70 °C for 12 h. This complex was isolated in pure form by precipitation with diethyl ether. Encapsulation was signaled by the disappearance of the ¹H NMR

peaks of free **1** and the concurrent appearance of a new set of peaks for the tetrahedron and its CRY guest, which were shifted upfield. All signals had the same diffusion coefficient (Figure 1c), which correspond to the CRY⊂**1** complex. As enantiomers of both **1** and CRY were present, and no diastereomeric species were observed by NMR after host-guest complexation, we infer stereoselective encapsulation to have taken place, forming a mixture of two enantiomeric host-guest complexes, which we infer to be *PP*-CRY⊂Δ_4-**1** and *MM*-CRY⊂Λ_4-**1** from the crystal structure discussed below. NOESY and ESI-MS spectra further indicated the formation of the 1:1 host-guest complex (Figures S19 and S23). The binding constant of **1** for CRY was too high to be determined directly; we thus employed di(p-tolyl)fluorine as an intermediate guest (Figure S24), allowing the determination of K_a = (9.5±0.4)×10^6 M^{-1} through competitive guest displacement (Figure S27).

We then tested the binding ability of the host-in-host complex, CRY⊂**1**, for the cesium cation, which is a known guest of other cryptophanes.[14] Slow vapor diffusion of ethyl acetate into an acetonitrile solution of a mixture of CRY⊂**1** and $CsCB_{11}H_{12}$ provided crystals suitable for X-ray crystallographic analysis (Figure 2). Carborate was used as the counter-anion of Cs^+ in order to obtain X-ray quality crystals.[15] Two enantiomers, [Cs^+⊂*PP*-CRY]⊂Δ_4-**1** and [Cs^+⊂*MM*-CRY]⊂Λ_4-**1**, are present in the unit cell (Figure S13). A single Cs^+ cation is located close to the centroid of the CRY cage with an average refined occupancy of 36%. Each $Fe^{II}_4L_4$ cage encapsulates a CRY in its cavity, displaying contacts consistent with the presence of CH-π interactions. The structure provided unambiguous assignment of the relative stereochemical orientations of the triazatruxene faces and tris-chelated octahedral vertices within **1**. The iron(II) centers are separated by distances of 20.0-20.9 Å. The volume of the central cavity was calculated to be 1010 and 913 $Å^3$ for the two crystallographically independent cages in the asymmetric unit (Figure S15). The degree of outward bending of some triazatruxene faces and the number of their internally oriented

ethyl groups accounted for the different volumes. The cavity was thus suitable for the accommodation of a CRY guest with an estimated volume of 694 Å^3.
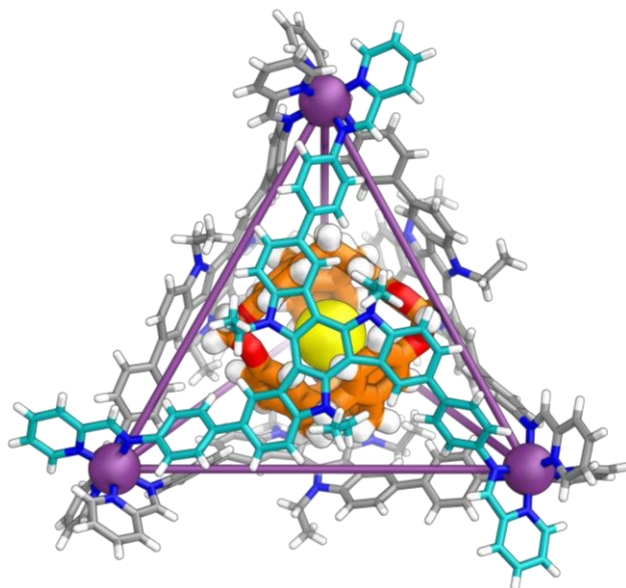

Figure 2. Crystal structure of [Cs$^+$⊂CRY]⊂**1** illustrating the [Cs$^+$⊂*PP*-CRY]⊂*Δ$_4$*-**1** enantiomer. The bound Cs$^+$, CRY and the front triazatruxene face are colored yellow, orange and cyan, respectively. Disorder, unbound counterions, and solvent of crystallization are omitted for clarity and only one of the two crystallographically independent complexes is shown.

Cesium binding by CRY⊂**1** was also observed in solution, in slow exchange on the NMR timescale. In this case, cesium triflimide was employed in order to match the counter-anions of the assembled cage. Upon progressive addition of CsNTf$_2$ to an acetonitrile solution of CRY⊂**1**, the initial ^{1}H NMR peaks gradually diminished with the appearance of a new set of signals corresponding to [Cs$^+$⊂CRY]⊂**1**, allowing a binding constant of 34±3 M^{-1} to be determined (Figure S28). The other alkali metal ions, including Li$^+$, Na$^+$, K$^+$, and Rb$^+$, were also tested, with no binding observed by ^{1}H NMR spectroscopy (Figure S29). Encapsulation of cesium was also demonstrated by ^{133}Cs NMR experiments. As shown in Figure 3a, after addition of Cs$^+$, a new peak appeared at -316 ppm alongside the free Cs$^+$ peak at 32 ppm. This new peak was assigned to the Cs$^+$ inside CRY⊂**1**, experiencing a strong shielding effect.[14] In contrast, without the outer tetrahedral host,

CRY was observed to bind Cs^+ in fast exchange on the NMR timescale, showing gradual shifts of the host proton signals during titrations (binding constant, 23 ± 1 M^{-1}) and only a single ^{133}Cs peak (Figures S34 and S35). The binding behavior of CRY had thus been altered through encapsulation, increasing the barrier to Cs^+ exchange and bringing about a slight amplification in binding strength. This enhancement in Cs^+ binding is counterintuitive, because the binding of CRY within **1** results in an 8+ charge surrounding the CRY-bound cesium cation. [$Cs^+\subset CRY$]$\subset$**1** thus represents an unusual example of encapsulation of a charged species within a capsule of the same charge.[16]
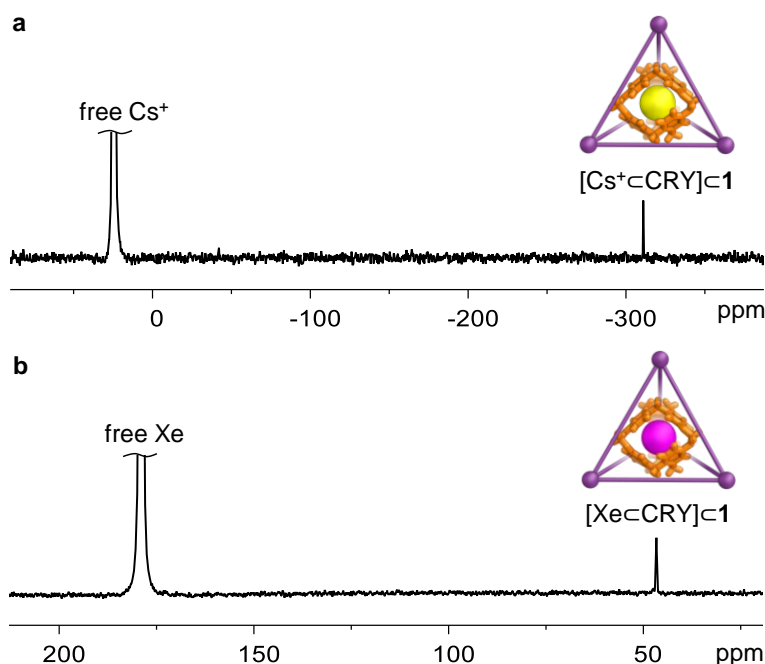

Figure 3. (a) ^{133}Cs NMR (CD_3CN, 66 MHz, 60 °C) spectrum of CRY$\subset$**1** in the presence of excess Cs^+. (b) ^{129}Xe NMR (CD_3CN, 138 MHz, 25 °C) spectrum of CRY$\subset$**1** in the presence of excess Xe.

Bubbling xenon gas through an acetonitrile solution of CRY$\subset$**1** also resulted in clear changes to its ^1H NMR spectrum (Figure S36), which were particularly significant in the region of the bound CRY, indicating encapsulation of Xe by CRY$\subset$**1**. ^{129}Xe NMR experiments using hyperpolarized Xe were then carried out. As shown in Figure 3b, in addition to the peak assigned to free Xe at 179 ppm, a new upfield peak at 47 ppm was observed, corresponding to Xe within CRY$\subset$**1**.

Addition of excess CRY into the same sample gave rise to another peak of CRY-caged xenon, at 50 ppm with much weaker intensity due to the low solubility of CRY in acetonitrile (Figure S37). The outer tetrahedral layer thus contributes to the shielding effect experienced by caged xenon, in addition to the CRY core. 1D selective inversion ^{129}Xe EXSY experiments with variable mixing time gave an exchange rate between [Xe⊂CRY]⊂**1** and free Xe of 11±2 Hz (Figure S38).[17]

We then set about investigating stereochemical communication between **1** and CRY in their host-guest complex (Figure 4). After adding enantiopure *PP*-CRY to **1** and heating to 70 °C for 12 h, two diastereomeric host-guest complexes, *PP*-CRY⊂*Δ*₄-**1** and *PP*-CRY⊂*Λ*₄-**1**, formed in a 1:1 ratio, as indicated by the presence of two sets of signals in the ^{1}H NMR spectrum (Figure S39). Maintaining the mixture at 70 °C for a further three days resulted in no change in the ratio between the two diastereomers, consistent with a high energy barrier for diastereomer interconversion. After the removal of excess CRY in solution by precipitating the host-guest complexes with diethyl ether and redissolution in CD₃CN, selective release of *PP*-CRY from *Λ*₄-**1** was observed after three days at 25 °C, resulting in diastereomeric enrichment of *PP*-CRY⊂*Δ*₄-**1** (Figure 4 and Figure S39). A binding constant of (1.8±0.1)×10⁴ M⁻¹ between *PP*-CRY and *Λ*₄-**1** was determined from ^{1}H NMR integration (Supplementary section 7.1, Figure S40), which is 530 times smaller than the affinity of (9.5±0.4)×10⁶ M⁻¹ between *PP*-CRY and *Δ*₄-**1** noted above, indicating high enantioselectivity of binding.

Heating the initially-formed mixture of *PP*-CRY⊂*Λ*₄-**1** and *PP*-CRY⊂*Δ*₄-**1** to 150 °C for four hours in a microwave reactor, however, resulted in the conversion of the mixture to 97% *PP*-CRY⊂*Δ*₄-**1** (Figure S41). The high temperature required and complete inversion of the chirality of all vertices suggest a mechanism of conversion involving a significant degree of cage disassembly and reassembly. Starting from *MM*-CRY resulted in the formation of the enantiomeric cage-in-cage product, *MM*-CRY⊂*Λ*₄-**1**, in a comparable yield (Figure S42). These enantiopure Russian doll precursors were isolated and purified by precipitation with diethyl ether. We infer that this

efficient stereochemical information transfer[18] reflects the high degree of enantioselectivity in binding between *PP*-CRY and the two enantiomers of *rac*-**1**.
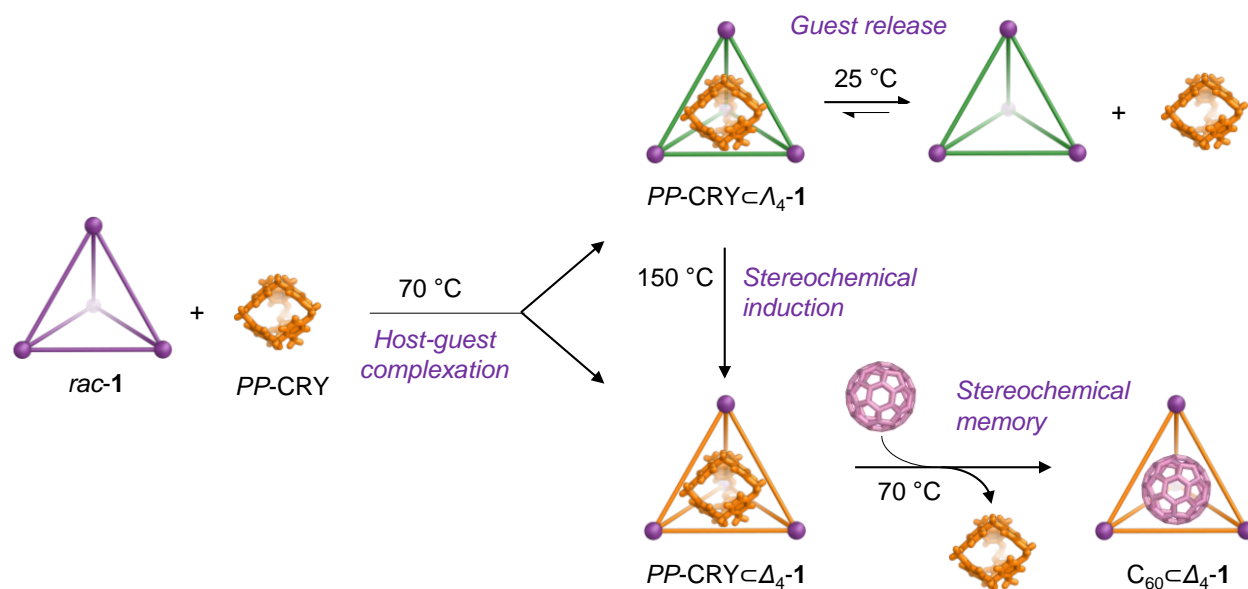

Figure 4. Stereochemical information transfer from CRY to **1**. The presence of excess *PP*-CRY and racemic **1** at 70 °C produced two diastereomeric host-guest complexes, but *PP*-CRY⊂Λ_4-**1** was observed to spontaneously lose guest at 25 °C after removal of excess CRY, and converted to the more stable *PP*-CRY⊂Δ_4-**1** upon heating to 150 °C. Subsequent treatment with C_{60} resulted in displacement of chiral CRY but maintenance of the stereochemical definition of **1**.

CD spectroscopy also confirmed stereochemical communication within the CRY⊂**1** system. As shown in Figure 5a, strong Cotton effects in the triazatruxene absorption region (300-350 nm) and for metal-to-ligand charge-transfer (MLCT) (500-650 nm) were observed in CD spectra of the host-guest complexes when using enantiopure CRY. The positive CD MLCT band corresponds to induction of Δ handedness of the metal center by *PP*-CRY, as observed in the crystal structure. This assignment is also consistent with previous observations.[13] No optical activity was observed when *rac*-CRY was used as the guest.

When achiral fullerene C_{60} displaced chiral CRY within **1** (Figures S43 and S44), strong Cotton effects as well as the sign, in particular of the MLCT region, persisted in the CD spectrum of the

new $C_{60} \subset \mathbf{1}$ host-guest complex (Figure 5b), suggesting a stereochemical memory effect.[13] No decrease in the intensity of the CD signals was observed after a month in solution (13 µM) at room temperature (Figure S45). We infer that the persistent stereochemical memory is a consequence of the structural integrity of the whole tetrahedral framework. This integrity is maintained by the rigid tritopic ligands of $\mathbf{1}$ during guest displacement, allowing this process to proceed without racemization.[13]
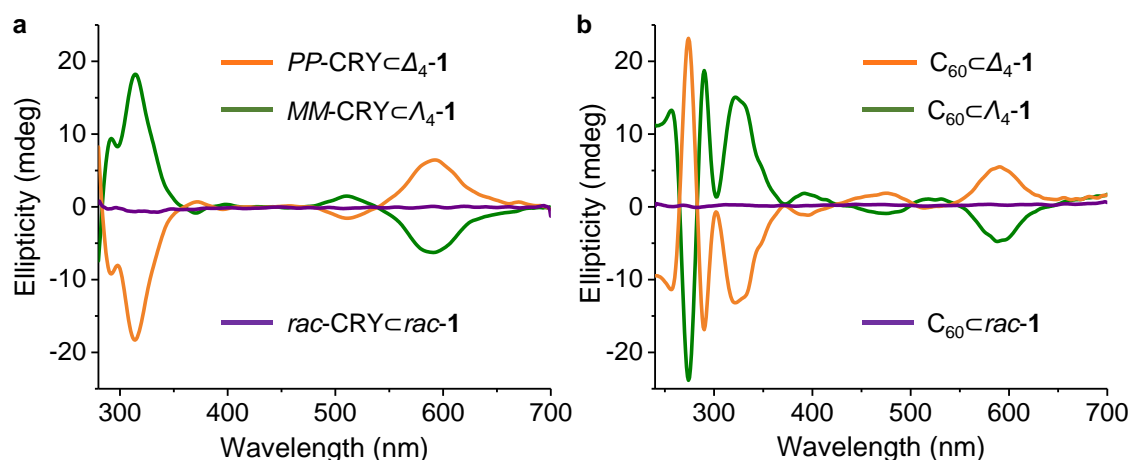

Figure 5. (a) CD spectra of PP-CRY$\subset\Delta_4$-**1** (orange), MM-CRY$\subset\Lambda_4$-**1** (green) and rac-CRY$\subset rac$-**1** (purple). (b) CD spectra of $C_{60}\subset\Delta_4$-**1** (orange), $C_{60}\subset\Lambda_4$-**1** (green) and $C_{60}\subset rac$-**1** (purple), formed following CRY guest displacement.

Addition of Cs^+ or xenon to the enantiopure cage-in-cage complexes allowed us to construct enantiopure three-component Russian dolls, $[Cs^+/Xe\subset PP\text{-}CRY]\subset\Delta_4$-**1** and $[Cs^+/Xe\subset MM\text{-}CRY]\subset\Lambda_4$-**1** (Figures S49 and S50). Cs^+ was able to serve as a probe to discriminate between diastereomeric complexes by NMR. Its addition to a solution containing the two diastereomers PP-CRY$\subset\Delta_4$-**1** and PP-CRY$\subset\Lambda_4$-**1** gave a ^{133}Cs NMR spectrum with peaks at 256 and 311 ppm (Figure 6a). Similarly, bubbling xenon into a solution of the same two diastereomeric nested hosts gave a ^{129}Xe NMR spectrum with host-guest resonances at 47 and 54 ppm. (Figure 6b). The ^{133}Cs and ^{129}Xe nuclei thus were able to sense the chirality of the outermost cage, even though the inner CRY cage was always of PP stereochemistry.[14,19] Moreover, the peak of xenon

encapsulated within CRY alone is located at 50 ppm (Figure S37), between the above two diastereomeric Xe signals, indicating that the outer capsule **1** is capable of either strengthening or weakening the shielding effect of the inner CRY core, depending on its stereochemistry.
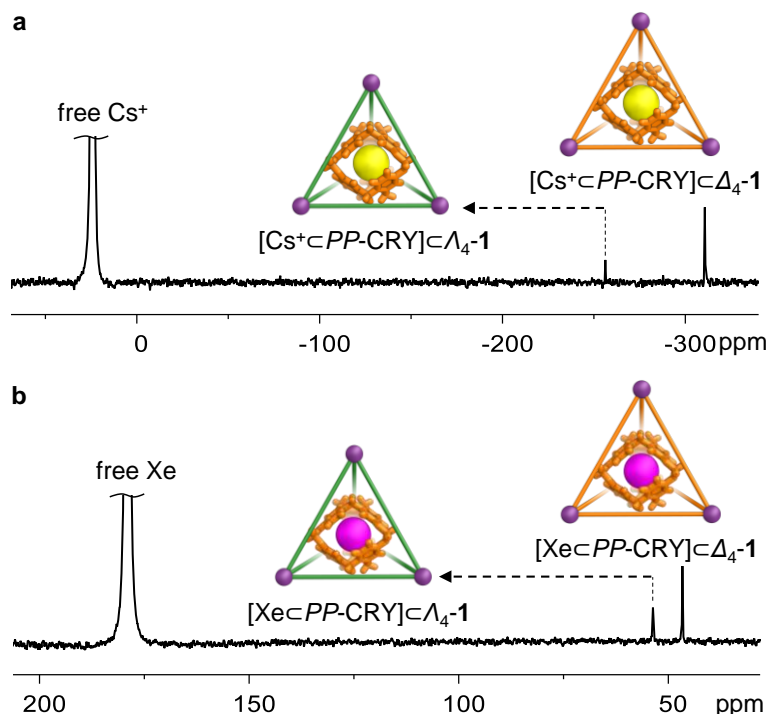

Figure 6. (a) ^{133}Cs NMR (CD$_3$CN, 66 MHz, 60 °C) spectrum of CRY⊂**1** containing the two diastereomers *PP*-CRY⊂*Δ*$_4$-**1** and *PP*-CRY⊂*Λ*$_4$-**1** in the presence of excess Cs$^+$. (b) ^{129}Xe NMR (CD$_3$CN, 138 MHz, 25 °C) spectrum of CRY⊂**1** containing two diastereomers *PP*-CRY⊂*Δ*$_4$-**1** and *PP*-CRY⊂*Λ*$_4$-**1** in the presence of excess Xe. In both NMR spectra, the peaks of encapsulated guests within *PP*-CRY⊂*Δ*$_4$-**1** are of higher intensity than those within *PP*-CRY⊂*Λ*$_4$-**1** due to the release of more weakly-bound *PP*-CRY from *Λ*$_4$-**1** during the NMR measurement (Figure S39).

Conclusion

The new [guest⊂cage]⊂cage complexes presented herein comprise a new class of enantiopure Russian dolls, building upon the foundations of previous host-in-host complexes involving two-dimensional macrocycles.[1a-j,1l] As Cs$^+$ was initially bound by CRY in fast exchange on the NMR timescale and Xe was insufficiently encapsulated by the poorly acetonitrile-soluble CRY, our

results demonstrate that encapsulation of a host can improve its guest binding performance. Inner "functionalization" of the large cavity of **1** through binding of CRY also enabled the encapsulation of a cation within a capsule bearing a high positive charge. The stereochemical induction effect of CRY upon the framework of **1**, followed by the displacement of the chiral guest, also represents a novel means to fix the stereochemistry of a host framework. These phenomena could prove useful for molecular-recognition-based applications, such as catalysis, separations, drug delivery and sensing.

Associated Content

Supporting Information

The Supporting Information is available free of charge on the ACS Publications website.

Complete experimental details (PDF)

X-ray data for [Cs$^+$⊂CRY]⊂**1** (CCDC 1894903)

Author Information

Corresponding Author

*J.N. jrn34@cam.ac.uk

ORCID

Dawei Zhang: 0000-0002-0898-9795

Tanya K. Ronson: 0000-0002-6917-3685

Jonathan R. Nitschke: 0000-0002-4060-5122

Acknowledgements

References

(1) (a) Parac, T. N.; Scherer, M.; Raymond, K. N. Host within a host: encapsulation of alkali ion-crown ether complexes into a $[Ga_4L_6]_{12}^-$ supramolecular cluster. *Angew. Chem. Int. Ed.* **2000**, *39*, 1239-1242; (b) Kim, S.-Y.; Jung, I.-S.; Lee, E.; Kim, J.; Sakamoto, S.; Yamaguchi, K.; Kim, K. Macrocycles within macrocycles: cyclen, cyclam, and their transition metal complexes encapsulated in cucurbit[8]uril. *Angew. Chem. Int. Ed.* **2001**, *40*, 2119-2121; (c) Kawase, T.; Tanaka, K.; Shiono, N.; Seirai, Y.; Oda, M. Onion-type complexation based on carbon nanorings and a buckminsterfullerene. *Angew. Chem. Int. Ed.* **2004**, *43*, 1722-1724; (d) Ueno, H.; Nishihara, T.; Segawa, Y.; Itami, K. Cycloparaphenylene-based ionic donor-acceptor supramolecule: isolation and characterization of $Li^+@C_{60}\subset[10]CPP$. *Angew. Chem. Int. Ed.* **2015**, *127*, 3778-3782; (e) Liu, S.; Zavalij, P. Y.; Isaacs, L. Cucurbit[10]uril. *J. Am. Chem. Soc.* **2005**, *127*, 16798-16799; (f) Shivanyuk, A. Nanoencapsulation of calix[4]arene inclusion complexes. *J. Am. Chem. Soc.* **2007**, *129*, 14196-14199; (g) Sawada, T.; Hisada, H.; Fujita, M. Mutual induced fit in a synthetic host-guest system. *J. Am. Chem. Soc.* **2014**, *136*, 4449-4451; (h) Cai, K.; Lipke, M. C.; Liu, Z.; Nelson, J.; Cheng, T.; Shi, Y.; Cheng, C.; Shen, D.; Han, J. M.; Vemuri, S.; Feng, Y.; Stern, C. L.; Goddard III, W. A.; Wasielewski, M. R.; Stoddart, J. F. Molecular Russian dolls. *Nat. Commun.* **2018**, *9*, 5275; (i) Danjo, H.; Hashimoto, Y.; Kidena, Y.; Nogamine, A.; Katagiri, K.; Kawahata, M.; Miyazawa, T.; Yamaguchi, K. Nestable tetrakis(spiroborate) nanocycles. *Org. Lett.* **2015**, *17*, 2154-2157; (j) Gong, W.; Yang, X.; Zavalij, P. Y.; Isaacs, L.; Zhao, Z.; Liu, S. From packed "sandwich" to "Russian doll": assembly by charge-transfer

interactions in cucurbit[10]uril. *Chem. Eur. J.* **2016**, *22*, 17612-17618; (k) Liu, Z.; Tian, C.; Yu, J.; Li, Y.; Jiang, W.; Mao, C. Self-assembly of responsive multilayered DNA nanocages. *J. Am. Chem. Soc.* **2015**, *137*, 1730-1733; (l) Lützen, A.; Renslo, A. R.; Schalley, C. A.; O'Leary, B. M.; Rebek, J. Encapsulation of ion-molecule complexes: second-sphere supramolecular chemistry. *J. Am. Chem. Soc.* **1999**, *121*, 7455-7456.

(2) (a) Day, A. I.; Blanch, R. J.; Arnold, A. P.; Lorenzo, S.; Lewis, G. R.; Dance, I. A cucurbituril-based syroscane: a new supramolecular form. *Angew. Chem. Int. Ed.* **2002**, *114*, 285-287; (b) Iwanaga, T.; Nakamoto, R.; Yasutake, M.; Takemura, H.; Sako, K.; Shinmyozu, T. Cyclophanes within cyclophanes: the synthesis of a pyromellitic diimide-based macrocycle as a structural unit in a molecular tube and its inclusion phenomena. *Angew. Chem. Int. Ed.* **2006**, *45*, 3643-3647; (c) Botana, E.; Da Silva, E.; Benet-Buchholz, J.; Ballester, P.; de Mendoza, J. Inclusion of cavitands and calix[4]arenes into a metallobridgedpara-(1H-imidazo[4,5-f][3,8]phenanthrolin-2-yl)-expanded calix[4]arene. *Angew. Chem. Int. Ed.* **2007**, *119*, 202-205; (d) Kaseborn, M.; Holstein, J. J.; Clever, G. H.; Lutzen, A. A rotaxane-like cage-in-ring structural motif for a metallosupramolecular Pd_6L_{12} aggregate. *Angew. Chem. Int. Ed.* **2018**, *57*, 12171-12175; (e) Bhat, I. A.; Samanta, D.; Mukherjee, P. S. A Pd_{24} pregnant molecular nanoball: self-templated stellation by precise mapping of coordination sites. *J. Am. Chem. Soc.* **2015**, *137*, 9497-9502; (f) Sun, B.; Wang, M.; Lou, Z.; Huang, M.; Xu, C.; Li, X.; Chen, L. J.; Yu, Y.; Davis, G. L.; Xu, B.; Yang, H. B.; Li, X. From ring-in-ring to sphere-in-sphere: self-assembly of discrete 2D and 3D architectures with increasing stability. *J. Am. Chem. Soc.* **2015**, *137*, 1556-1564.

(3) (a) Dalgarno, S. J.; Atwood, J. L.; Raston, C. L. Sulfonatocalixarenes: molecular capsule and 'Russian doll' arrays to structures mimicking viral geometry. *Chem. Commun.* **2006**, 4567-4574; (b) Hardie, M. J.; Raston, C. L. Russian doll assembled superanion capsule-metal ion complexes: combinatorial supramolecular chemistry in aqueous media. *Dalton Trans.* **2000**, 2483-2492.

(4) Rousseaux, S. A.; Gong, J. Q.; Haver, R.; Odell, B.; Claridge, T. D.; Herz, L. M.; Anderson, H. L. Self-assembly of Russian doll concentric porphyrin nanorings. *J. Am. Chem. Soc.* **2015**, *137*, 12713-12718.

(5) (a) Glasgow, J. E.; Capehart, S. L.; Francis, M. B.; Tullman-Ercek, D. Osmolyte-mediated encapsulation of proteins inside MS2 viral capsids. *ACS Nano* **2012**, *6*, 8658-8664; (b) Peters, R. J. R. W.; Louzao, I.; van Hest, J. C. M. From polymeric nanoreactors to artificial organelles. *Chem. Sci.* **2012**, *3*, 335-

342; (c) Sairenji, S.; Akine, S.; Nabeshima, T. Response speed control of helicity inversion based on a "regulatory enzyme"-like strategy. *Sci. Rep.* **2018**, *8*, 137; (d) Zhang, Q.; Catti, L.; Tiefenbacher, K. Catalysis inside the hexameric resorcinarene capsule. *Acc. Chem. Res.* **2018**, *51*, 2107-2114; (e) Juricek, M.; Strutt, N. L.; Barnes, J. C.; Butterfield, A. M.; Dale, E. J.; Baldridge, K. K.; Stoddart, J. F.; Siegel, J. S. Induced-fit catalysis of corannulene bowl-to-bowl inversion. *Nature Chem.* **2014**, *6*, 222-228.

(6) Byrne, K.; Zubair, M.; Zhu, N.; Zhou, X. P.; Fox, D. S.; Zhang, H.; Twamley, B.; Lennox, M. J.; Duren, T.; Schmitt, W. Ultra-large supramolecular coordination cages composed of endohedral Archimedean and Platonic bodies. *Nat. Commun.* **2017**, *8*, 15268.

(7) (a) Cook, T. R.; Stang, P. J. Recent developments in the preparation and chemistry of metallacycles and metallacages via coordination. *Chem. Rev.* **2015**, *115*, 7001-7045; (b) Zhang, D.; Ronson, T. K.; Nitschke, J. R. Functional capsules via subcomponent self-assembly. *Acc. Chem. Res.* **2018**, *51*, 2423-2436; (c) Custelcean, R.; Bonnesen, P. V.; Duncan, N. C.; Zhang, X.; Watson, L. A.; Van Berkel, G.; Parson, W. B.; Hay, B. P. Urea-functionalized M_4L_6 cage receptors: anion-templated self-assembly and selective guest exchange in aqueous solutions. *J. Am. Chem. Soc.* **2012**, *134*, 8525-8534; (d) Ward, M. D.; Hunter, C. A.; Williams, N. H. Coordination cages based on bis(pyrazolylpyridine) ligands: structures, dynamic behavior, guest Binding, and catalysis. *Acc. Chem. Res.* **2018**, *51*, 2073-2082; (e) Zhou, X. P.; Wu, Y.; Li, D. Polyhedral metal-imidazolate cages: control of self-assembly and cage to cage transformation. *J. Am. Chem. Soc.* **2013**, *135*, 16062-16065; (f) Yamashina, M.; Kusaba, S.; Akita, M.; Kikuchi, T.; Yoshizawa, M. Cramming versus threading of long amphiphilic oligomers into a polyaromatic capsule. *Nat. Commun.* **2018**, *9*, 4227; (g) Preston, D.; Sutton, J. J.; Gordon, K. C.; Crowley, J. D. A nona-nuclear heterometallic Pd_3Pt_6 "donut"-shaped cage: molecular recognition and photocatalysis. *Angew. Chem. Int. Ed.* **2018**, *57*, 8659-8663; (h) Burke, B. P.; Grantham, W.; Burke, M. J.; Nichol, G. S.; Roberts, D.; Renard, I.; Hargreaves, R.; Cawthorne, C.; Archibald, S. J.; Lusby, P. J. Visualizing kinetically robust $Co^{III}_4L_6$ assemblies in vivo: SPECT imaging of the encapsulated [^{99m}Tc]TcO$_4^-$ Anion. *J. Am. Chem. Soc.* **2018**, *140*, 16877-16881; (i) Dolinar, B. S.; Alexandropoulos, D. I.; Vignesh, K. R.; James, T.; Dunbar, K. R. Lanthanide triangles supported by radical bridging ligands. *J. Am. Chem. Soc.* **2018**, *140*, 908-911; (j) Kim, J.; Lee, D. Crisscrossing coordination networks: ligand doping to control the chemomechanical properties of stimuli-responsive metallogels. *Chem. Sci.* **2019**, *10*, 3864-3872.

(8) (a) Mauro, M.; Aliprandi, A.; Septiadi, D.; Kehr, N. S.; De Cola, L. When self-assembly meets biology: luminescent platinum complexes for imaging applications. *Chem. Soc. Rev.* **2014**, *43*, 4144-4166; (b) Chan, A. K.; Lam, W. H.; Tanaka, Y.; Wong, K. M.; Yam, V. W. Multiaddressable molecular rectangles with reversible host-guest interactions: modulation of pH-controlled guest release and capture. *Proc. Natl. Acad. Sci. U. S. A.* **2015**, *112*, 690-695; (c) Leigh, D. A.; Pritchard, R. G.; Stephens, A. J. A Star of David catenane. *Nature Chem.* **2014**, *6*, 978-982; (d) Pramanik, S.; Aprahamian, I. Hydrazone switch-based negative feedback loop. *J. Am. Chem. Soc.* **2016**, *138*, 15142-15145; (e) Barry, D. E.; Caffrey, D. F.; Gunnlaugsson, T. Lanthanide-directed synthesis of luminescent self-assembly supramolecular structures and mechanically bonded systems from acyclic coordinating organic ligands. *Chem. Soc. Rev.* **2016**, *45*, 3244-3274; (f) Wei, P.; Yan, X.; Huang, F. Supramolecular polymers constructed by orthogonal self-assembly based on host-guest and metal-ligand interactions. *Chem. Soc. Rev.* **2015**, *44*, 815-832; (g) Yang, L.; Tan, X.; Wang, Z.; Zhang, X. Supramolecular polymers: historical development, preparation, characterization, and functions. *Chem. Rev.* **2015**, *115*, 7196-7239; (h) Akine, S.; Miyashita, M.; Nabeshima, T. A metallo-molecular cage that can close the apertures with coordination bonds. *J. Am. Chem. Soc.* **2017**, *139*, 4631-4634; (i) Garcia-Simon, C.; Garcia-Borras, M.; Gomez, L.; Parella, T.; Osuna, S.; Juanhuix, J.; Imaz, I.; Maspoch, D.; Costas, M.; Ribas, X. Sponge-like molecular cage for purification of fullerenes. *Nat. Commun.* **2014**, *5*, 5557; (j) Ozores, H. L.; Amorin, M.; Granja, J. R. Self-assembling molecular capsules based on α,γ-cyclic Peptides. *J. Am. Chem. Soc.* **2017**, *139*, 776-784.

(9) Brotin, T.; Dutasta, J. P. Cryptophanes and their complexes-present and future. *Chem. Rev.* **2009**, *109*, 88-130.

(10) Hardie, M. J. Recent advances in the chemistry of cyclotriveratrylene. *Chem. Soc. Rev.* **2010**, *39*, 516-527.

(11) (a) Fogarty, H. A.; Berthault, P.; Brotin, T.; Huber, G.; Desvaux, H.; Dutasta, J. P. A cryptophane core optimized for xenon encapsulation. *J. Am. Chem. Soc.* **2007**, *129*, 10332-10333; (b) Buffeteau, T.; Pitrat, D.; Daugey, N.; Calin, N.; Jean, M.; Vanthuyne, N.; Ducasse, L.; Wien, F.; Brotin, T. Chiroptical properties of cryptophane-111. *Phys. Chem. Chem. Phys.* **2017**, *19*, 18303-18310.

(12) (a) Wang, X.; Wang, Y.; Yang, H.; Fang, H.; Chen, R.; Sun, Y.; Zheng, N.; Tan, K.; Lu, X.; Tian, Z.; Cao, X. Assembled molecular face-rotating polyhedra to transfer chirality from two to three dimensions.

Nat. Commun. **2016**, *7*, 12469; (b) Wang, Y.; Fang, H.; Tranca, I.; Qu, H.; Wang, X.; Markvoort, A. J.; Tian, Z.; Cao, X. Elucidation of the origin of chiral amplification in discrete molecular polyhedra. *Nat. Commun.* **2018**, *9*, 488.

(13) Castilla, A. M.; Ousaka, N.; Bilbeisi, R. A.; Valeri, E.; Ronson, T. K.; Nitschke, J. R. High-fidelity stereochemical memory in a Fe$^{II}_4$L$_4$ tetrahedral capsule. *J. Am. Chem. Soc.* **2013**, *135*, 17999-18006.

(14) Brotin, T.; Montserret, R.; Bouchet, A.; Cavagnat, D.; Linares, M.; Buffeteau, T. High affinity of water-soluble cryptophanes for cesium cations. *J. Org. Chem.* **2012**, *77*, 1198-1201.

(15) Rizzuto, F. J.; Nitschke, J. R. Stereochemical plasticity modulates cooperative binding in a Co$^{II}_{12}$L$_6$ cuboctahedron. *Nature Chem.* **2017**, *9*, 903.

(16) (a) Bourgeois, J. P.; Fujita, M.; Kawano, M.; Sakamoto, S.; Yamaguchi, K. A cationic guest in a 24+ cationic host. *J. Am. Chem. Soc.* **2003**, *125*, 9260-9261; (b) Bruns, C. J.; Fujita, D.; Hoshino, M.; Sato, S.; Stoddart, J. F.; Fujita, M. Emergent ion-gated binding of cationic host-guest complexes within cationic M$_{12}$L$_{24}$ molecular flasks. *J. Am. Chem. Soc.* **2014**, *136*, 12027-12034; (c) Zhang, L.; Schmitt, W. From platonic templates to Archimedean solids: successive construction of nanoscopic {V$_{16}$As$_8$}, {V$_{16}$As$_{10}$}, {V$_{20}$As$_8$}, and {V$_{24}$As$_8$} polyoxovanadate cages. *J. Am. Chem. Soc.* **2011**, *133*, 11240-11248.
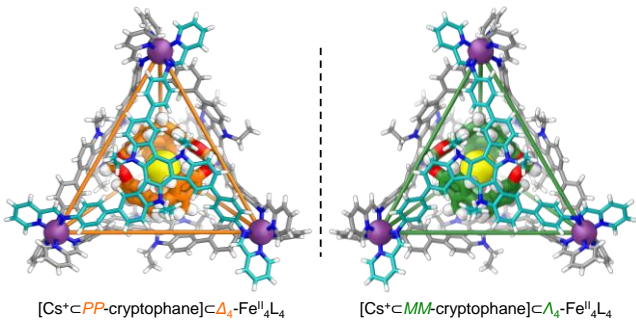
(17) Roukala, J.; Zhu, J.; Giri, C.; Rissanen, K.; Lantto, P.; Telkki, V. V. Encapsulation of xenon by a self-assembled Fe$_4$L$_6$ metallosupramolecular cage. *J. Am. Chem. Soc.* **2015**, *137*, 2464-2467.

(18) (a) Beaudoin, D.; Rominger, F.; Mastalerz, M. Chirality-assisted synthesis of a very large octameric hydrogen-bonded capsule. *Angew. Chem. Int. Ed.* **2016**, *55*, 15599-15603; (b) Kinney, Z. J.; Hartley, C. S. Twisted macrocycles with folded ortho-phenylene subunits. *J. Am. Chem. Soc.* **2017**, *139*, 4821-4827; (c) Van Craen, D.; Albrecht, M.; Raabe, G.; Pan, F.; Rissanen, K. A supramolecular chiral auxiliary approach: "remote control" of stereochemistry at a hierarchically assembled dimeric helicate. *Chem. Eur. J.* **2016**, *22*, 3255-3258; (d) Young, M. C.; Holloway, L. R.; Johnson, A. M.; Hooley, R. J. A supramolecular sorting hat: stereocontrol in metal-ligand self-assembly by complementary hydrogen bonding. *Angew. Chem. Int. Ed.* **2014**, *53*, 9832-9836; (e) Chen, L. J.; Yang, H. B.; Shionoya, M. Chiral metallosupramolecular architectures. *Chem. Soc. Rev.* **2017**, *46*, 2555-2576; (f) Tsunoda, Y.; Fukuta, K.; Imamura, T.; Sekiya, R.; Furuyama, T.; Kobayashi, N.; Haino, T. High diastereoselection of a dissymmetric capsule by chiral guest complexation. *Angew. Chem. Int. Ed.* **2014**, *53*, 7243-7247; (g) Han, X.; Zhang, J.; Huang, J.; Wu, X.; Yuan, D.; Liu, Y.;

Cui, Y. Chiral induction in covalent organic frameworks. *Nat. Commun.* **2018**, *9*, 1294; (h) Helmich, F.; Lee, C. C.; Schenning, A. P.; Meijer, E. W. Chiral memory via chiral amplification and selective depolymerization of porphyrin aggregates. *J. Am. Chem. Soc.* **2010**, *132*, 16753-16755; (i) Ikeda, M.; Tanaka, Y.; Hasegawa, T.; Furusho, Y.; Yashima, E. Construction of double-stranded metallosupramolecular polymers with a controlled helicity by combination of salt bridges and metal coordination. *J. Am. Chem. Soc.* **2006**, *128*, 6806-6807; (j) Kubo, Y.; Ohno, T.; Yamanaka, J.-i.; Tokita, S.; Iida, T.; Ishimaru, Y. Chirality-transfer control using a heterotopic zinc(II) porphyrin dimer. *J. Am. Chem. Soc.* **2001**, *123*, 12700-12701.

(19) Ruiz, E. J.; Sears, D. N.; Pines, A.; Jameson, C. J. Diastereomeric Xe chemical shifts in tethered cryptophane cages. *J. Am. Chem. Soc.* **2006**, *128*, 16980-16988.

1
2
3
4
5
6
7
8
9
10
11
12
13
14
15
16
17
18
19
20
21
22
23
24
25
26
27
28
29
30
31
32
33
34
35
36
37
38
39
40
41
42
43
44
45
46
47
48
49
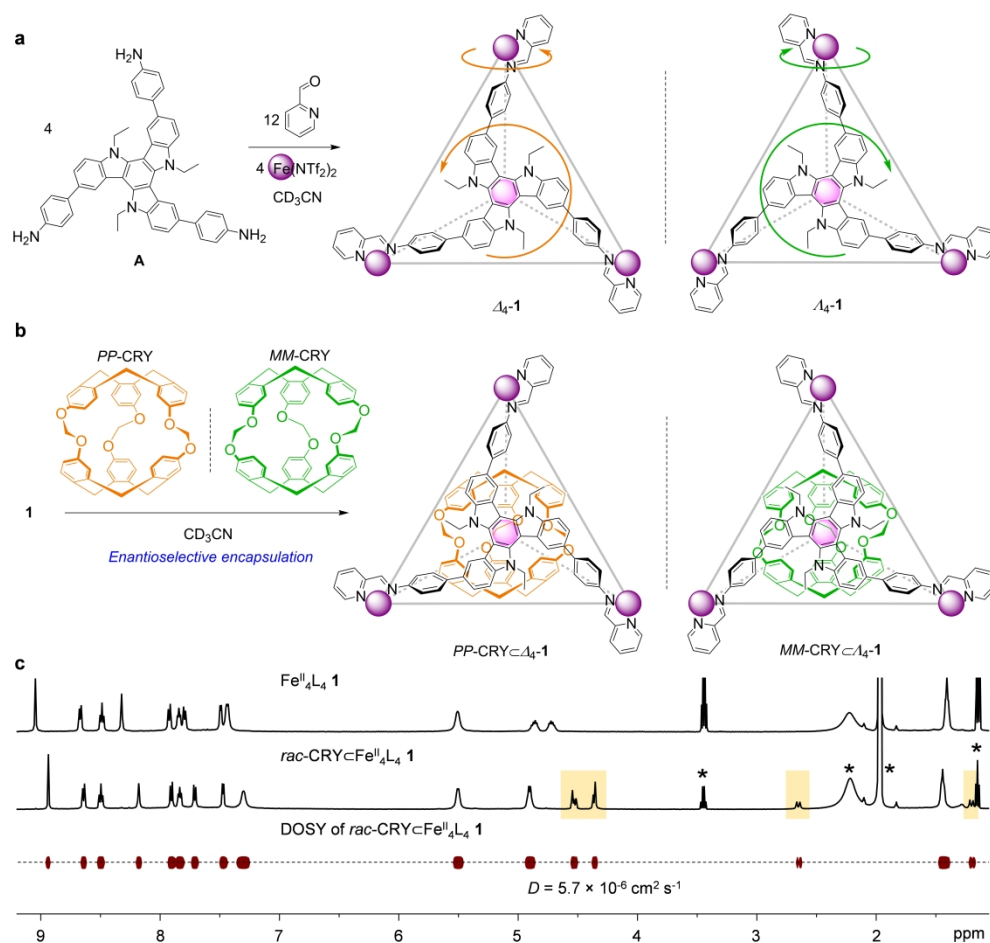50
51
52
53
54
55
56
57
58
59
60

Table of Contents artwork

$[Cs^+ \subset PP\text{-cryptophane}] \subset \Delta_4\text{-}Fe^{II}_4L_4$ $[Cs^+ \subset MM\text{-cryptophane}] \subset \Lambda_4\text{-}Fe^{II}_4L_4$

Figure 1. (a) Subcomponent self-assembly of 1. (b) Enantioselective encapsulation of rac-CRY by 1. (c) 1H NMR spectra (CD3CN, 500 MHz, 25 °C) of 1 and CRY⊂1, and DOSY spectrum of CRY⊂1. The peaks of the encapsulated CRY have been highlighted with a light orange background. Solvent peaks from diethyl ether, water and acetonitrile are indicated by asterisks. DOSY NMR indicated that the signals from 1 and the bound CRY diffuse at the same rate.
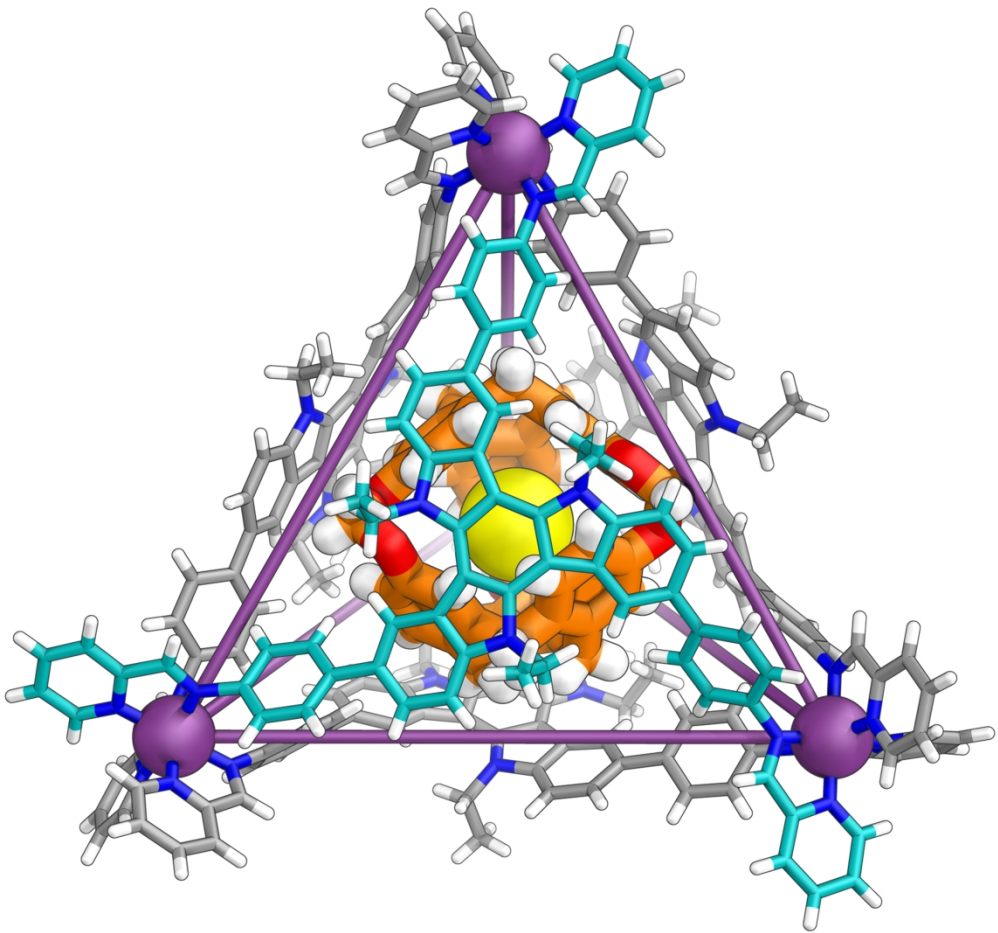
541x512mm (300 x 300 DPI)

Figure 2. Crystal structure of [Cs+⊂CRY]⊂1 illustrating the [Cs+⊂PP-CRY]⊂Δ4-1 enantiomer. The bound Cs+, CRY and the front triazatruxene face are colored yellow, orange and cyan, respectively. Disorder, unbound counterions, and solvent of crystallization are omitted for clarity and only one of the two crystallographically independent complexes is shown.
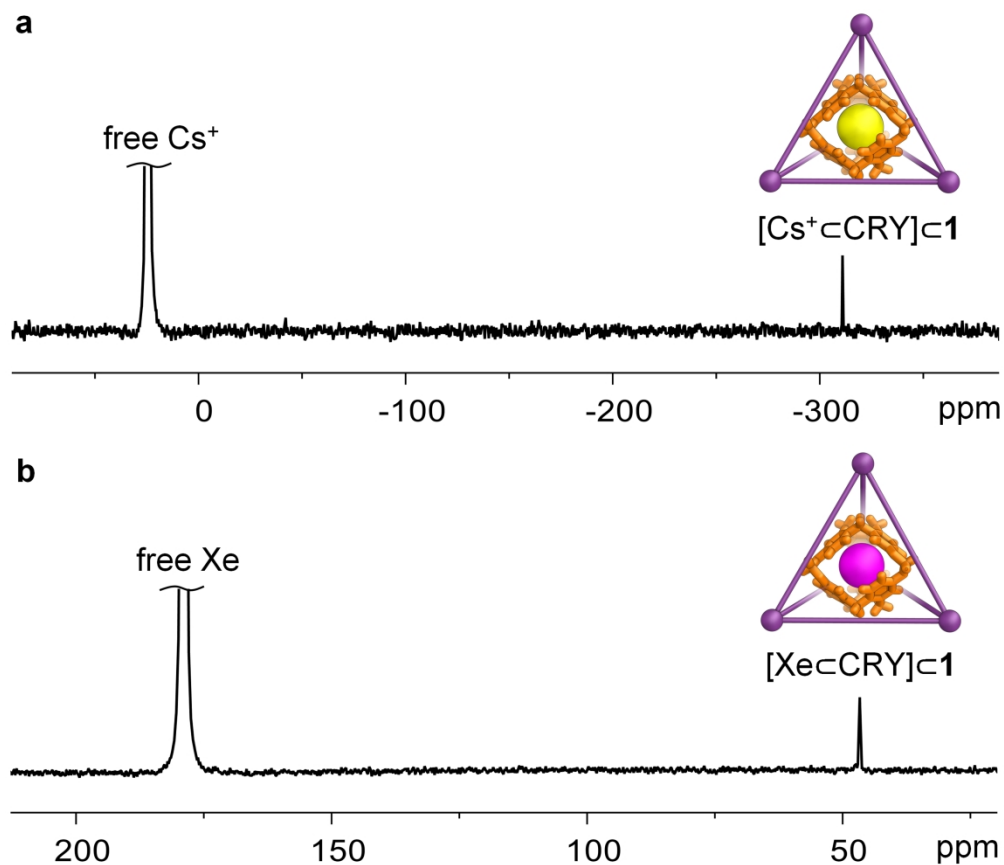
541x512mm (300 x 300 DPI)

Figure 3. (a) 133Cs NMR (CD3CN, 66 MHz, 60 °C) spectrum of CRY⊂1 in the presence of excess Cs+. (b) 129Xe NMR (CD3CN, 138 MHz, 25 °C) spectrum of CRY⊂1 in the presence of excess Xe.
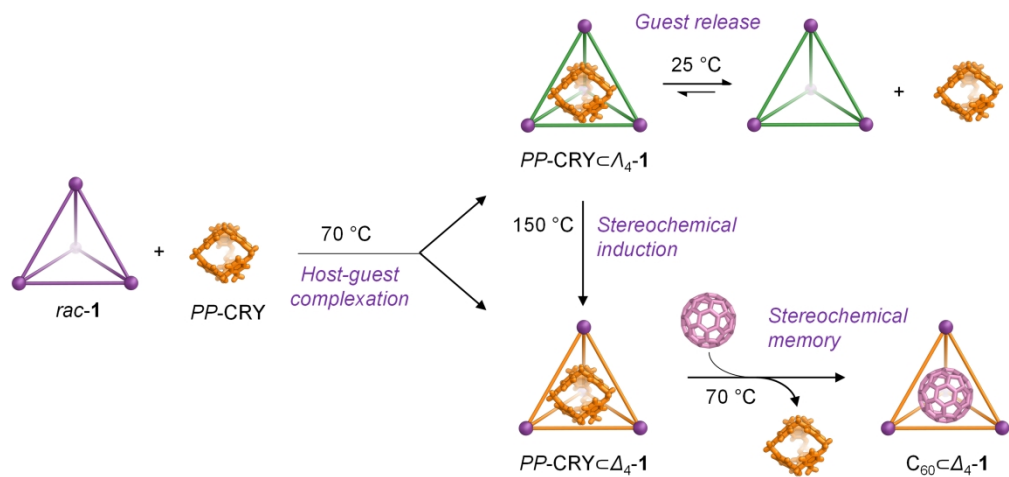
327x281mm (300 x 300 DPI)

Figure 4. Stereochemical information transfer from CRY to 1. The presence of excess PP-CRY and racemic 1 at 70 °C produced two diastereomeric host-guest complexes, but PP-CRY⊂Λ4-1 was observed to spontaneously lose guest at 25 °C after removal of excess CRY, and converted to the more stable PP-CRY⊂Δ4-1 upon heating to 150 °C. Subsequent treatment with C60 resulted in displacement of chiral CRY but maintenance of the stereochemical definition of 1.
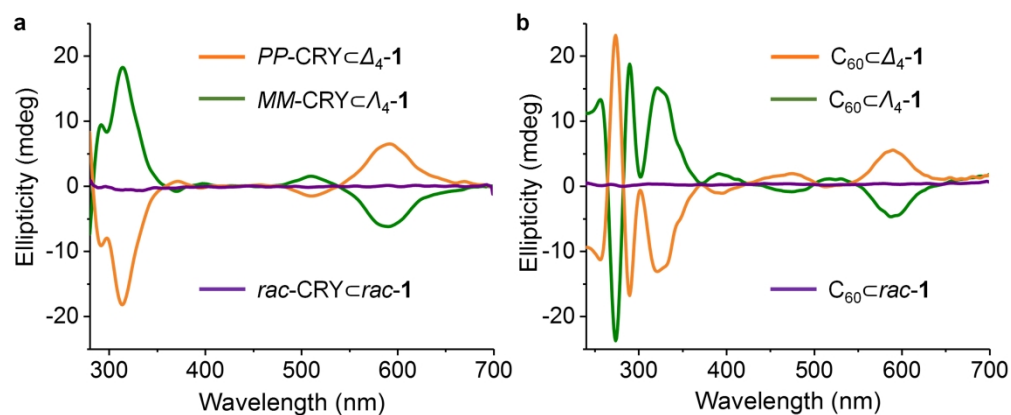
524x245mm (300 x 300 DPI)

Figure 5. (a) CD spectra of PP-CRY⊂Δ4-1 (orange), MM-CRY⊂Λ4-1 (green) and rac-CRY⊂rac-1 (purple). (b) CD spectra of C60⊂Δ4-1 (orange), C60⊂Λ4-1 (green) and C60⊂rac-1 (purple), formed following CRY guest displacement.

542x220mm (300 x 300 DPI)

a

b

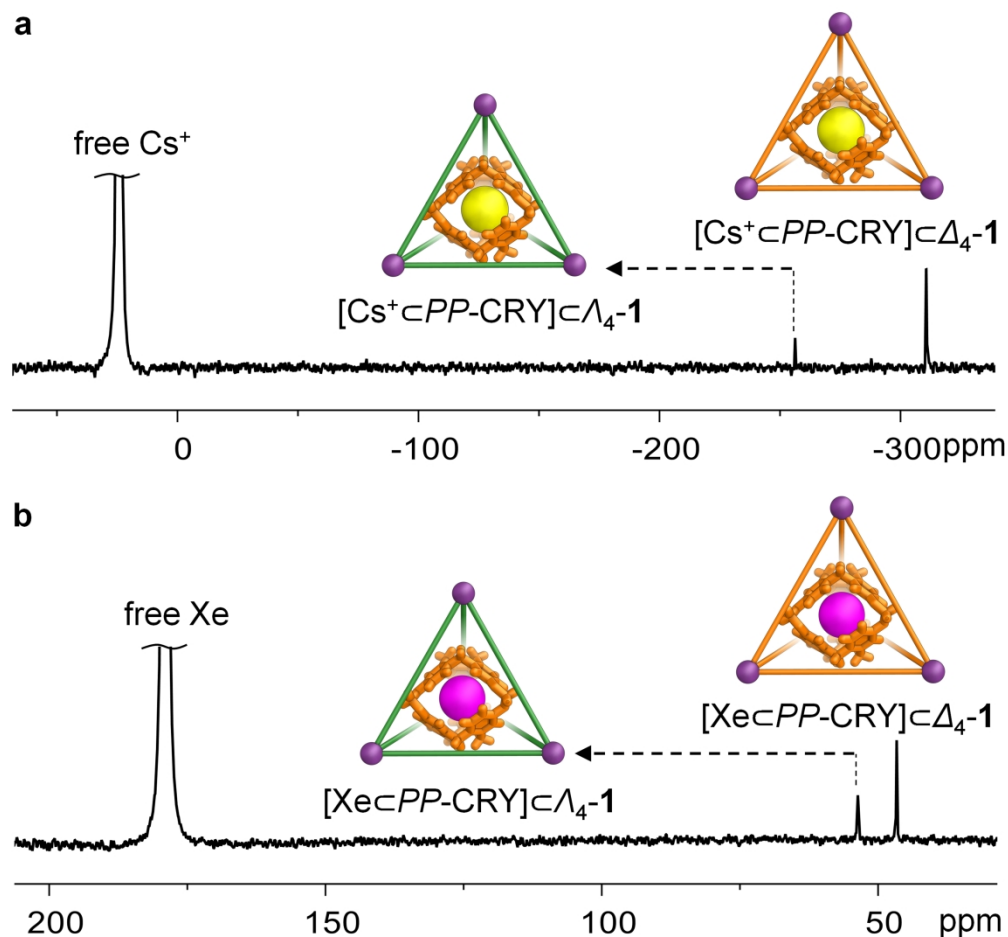

Figure 6. (a) 133Cs NMR (CD3CN, 66 MHz, 60 °C) spectrum of CRY⊂1 containing the two diastereomers PP-CRY⊂Δ4-1 and PP-CRY⊂Λ4-1 in the presence of excess Cs+. (b) 129Xe NMR (CD3CN, 138 MHz, 25 °C) spectrum of CRY⊂1 containing two diastereomers PP-CRY⊂Δ4-1 and PP-CRY⊂Λ4-1 in the presence of excess Xe. In both NMR spectra, the peaks of encapsulated guests within PP-CRY⊂Δ4-1 are of higher intensity than those within PP-CRY⊂Λ4-1 due to the release of more weakly-bound PP-CRY from Λ4-1 during the NMR measurement (Figure S39).

322x303mm (300 x 300 DPI)